ORIGINAL ARTICLE



Wavelength-Selective Fluorescence of a Model Transmembrane Peptide: Constrained Dynamics of Interfacial Tryptophan Anchors

Sreetama Pal 1,2 · Roger E. Koeppe II 3 · Amitabha Chattopadhyay 2,4

Received: 13 July 2018 / Accepted: 3 September 2018 / Published online: 17 September 2018 © Springer Science+Business Media, LLC, part of Springer Nature 2018

Abstract

WALPs are prototypical, α -helical transmembrane peptides that represent a consensus sequence for transmembrane segments of integral membrane proteins and serve as excellent models for exploring peptide-lipid interactions and hydrophobic mismatch in membranes. Importantly, the WALP peptides are in direct contact with the lipids. They consist of a central stretch of alternating hydrophobic alanine and leucine residues capped at both ends by tryptophans. In this work, we employ wavelength-selective fluorescence approaches to explore the intrinsic fluorescence of tryptophan residues in WALP23 in 1-palmitoyl-2-oleoyl-sn-glycero-3-phosphocholine (POPC) membranes. Our results show that the four tryptophan residues in WALP23 exhibit an average red edge excitation shift (REES) of 6 nm, implying their localization at the membrane interface, characterized by a restricted microenvironment. This result is supported by fluorescence anisotropy and lifetime measurements as a function of wavelength displayed by WALP23 tryptophans in POPC membranes. These results provide a new approach based on intrinsic fluorescence of interfacial tryptophans to address protein-lipid interaction and hydrophobic mismatch.

Keywords WALP · Interfacial tryptophan anchor · REES · Hydrophobic mismatch

Introduction

Short transmembrane model peptides have proved to be useful in addressing the complex interplay between proteins and lipids in the membrane milieu, including lipid-protein and protein-protein interactions [1]. In this context, model peptides belonging to the WALP family, represented by the general sequence acetyl-GWW-(LA)_n-LWWA-ethanolamide (see Fig. 1), have emerged as a popular choice for understanding peptide orientation, dynamics, hydrophobic mismatch and

Electronic supplementary material The online version of this article (https://doi.org/10.1007/s10895-018-2293-5) contains supplementary material, which is available to authorized users.

- Amitabha Chattopadhyay amit@ccmb.res.in
- CSIR-Indian Institute of Chemical Technology, Uppal Road, Hyderabad 500 007, India
- Academy of Scientific and Innovative Research, Ghaziabad, India
- Department of Chemistry and Biochemistry, University of Arkansas, Fayetteville, AR 72701, USA
- CSIR-Centre for Cellular and Molecular Biology, Uppal Road, Hyderabad 500 007, India

lipid phase behavior [2–5]. WALPs are prototypical, α helical transmembrane peptides, modeled on the hydrophobic channel-forming peptide, gramicidin [6–8]. WALP peptides consist of a central stretch of alternating hydrophobic alanine and leucine residues capped at both ends by two tryptophans. Both alanine and leucine have a high propensity for assuming α-helical conformation and the number of Ala-Leu repeats can be varied to tune the hydrophobic length of the peptide. Due to this characteristic sequence, WALPs represent a consensus, albeit simplified, motif for representing transmembrane α -helical segments of intrinsic membrane proteins. The representation is appropriate because transmembrane segments of integral membrane proteins are understood as consisting of predominantly hydrophobic α -helical stretches, flanked by a 'belt' of aromatic or charged residues at each end [9, 10]. Interestingly, the WALP helices are tilted in the membrane [4, 11, 12]. Importantly, interfacially localized tryptophan residues are known to be crucial in maintaining protein functionality and in defining the protein hydrophobic length by acting as membrane anchors [13, 14].

The suitability of WALPs as a model system for investigating hydrophobic mismatch in membranes has been established by Killian, Koeppe and co-workers, predominantly utilizing nuclear magnetic resonance (NMR) approaches.



Hydrophobic mismatch refers to a particular type of lipidprotein interaction in which the hydrophobic part (length) of a transmembrane segment of a membrane protein (or peptide) does not match the hydrophobic thickness of the membrane bilayer in which it is embedded [15-19]. Hydrophobic mismatch conditions induced by WALPs have been reported to trigger the formation of non-bilayer structures in model membranes [2, 20] and in membranes mimicking E. coli membranes [21]. The formation of non-lamellar phases in the presence of WALP helices is a consequence of the flanking tryptophan indole rings, which act as amphipathic membrane anchors and override the hydrophobic matching effects, a common response to mismatch conditions [22]. This lipid response to hydrophobic mismatch was found to be dependent on the nature of interfacial residues in WALP analogs [23, 24]. Due to the membrane-anchored structure of these peptides, the peptide response to hydrophobic mismatch was manifested as changes in tilt angles [4, 11, 25] and distortions in the helix [26], again dependent on the nature of the interfacial residues. In spite of these evidences highlighting the crucial role of the tryptophan anchors in WALP-membrane interactions, there have been very few reports on this aspect utilizing the microenvironment-sensitive window provided by the intrinsic

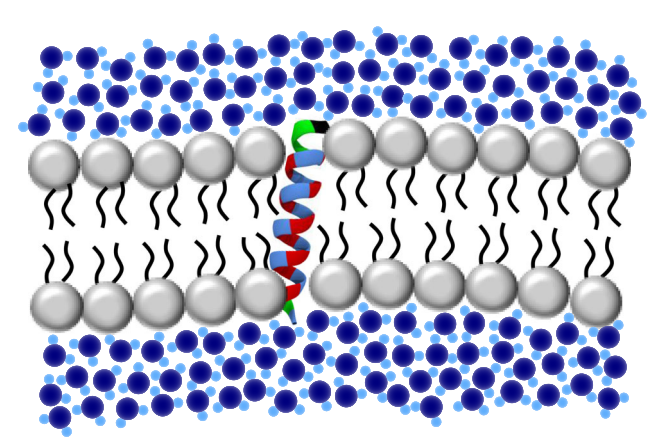
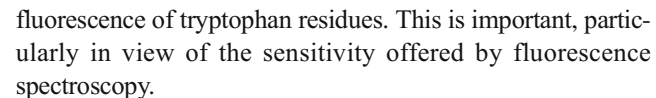


Fig. 1 A schematic showing the amino acid sequence (top) and membrane topology (bottom) of the model transmembrane peptide WALP23. WALPs are a class of synthetic peptides that consist of a core of alternating hydrophobic alanine and leucine residues (shown in blue and red, respectively), capped on each side by two tryptophans (marked in green). This characteristic sequence ensures that WALP peptides represent a consensus sequence for α -helical transmembrane domains of membrane proteins. The helix is tilted in the membrane [4], and the hydrophobic length of the peptide can be tuned by changing the number of alanine-leucine repeats, thereby making these peptides excellent systems for exploring signatures and consequences of hydrophobic mismatch in membranes. The phospholipid headgroups are depicted as gray beads and fatty acyl chains are shown in black. Water molecules are depicted in shades of blue. See text for more details



In this paper, we have applied wavelength-selective fluorescence approaches to explore the organization and dynamics of the membrane-anchoring tryptophans in WALP23, in the overall context of the fundamental role that tryptophan residues assume in the organization, dynamics, stability and function of several membrane peptides and proteins [13, 14, 27-30]. The red edge excitation shift (REES) toolbox represents an experimental approach that makes use of slow solvation dynamics of fluorophores in the excited state to photoselect fluorophore populations with varying degrees of solvation corresponding to each excitation wavelength. This powerful approach can be used to conveniently probe the solvation dynamics and fluorophore microenvironment in organized molecular assemblies such as membrane bilayers or folded proteins, which impose slow rates of solvent relaxation [31–34]. We report here that the tryptophan residues in WALP23 exhibit REES in model membranes, thereby indicating and confirming their localization at the membrane interface, characterized by restricted microenvironment. In addition, WALP23 tryptophans display changes in fluorescence anisotropy and lifetime as a function of wavelength, which reinforce these results. These results assume significance in the backdrop of the widely documented role of tryptophan residues in membrane protein structure and function, and in the specific context of tryptophan-mediated response of peptide helices to hydrophobic mismatch in lipid membranes.

Experimental

Materials

1-Palmitoyl-2-oleoyl-*sn*-glycero-3-phosphocholine (POPC) was obtained from Avanti Polar Lipids (Alabaster, AL). WALP23 was synthesized as described previously [2]. 1,2-Dimyristoyl-sn-glycero-3-phosphocholine (DMPC), Na₂HPO₄, NaH₂PO₄, and NaCl were purchased from Sigma Chemical Co. (St. Louis, MO). The concentration of peptide stocks in methanol was calculated utilizing a molar extinction coefficient (ϵ) of 22,400 M⁻¹ cm⁻¹ at 280 nm [35]. Silica gel pre-coated plates from Merck (Darmstadt, Germany) were used for checking lipid purity by thin layer chromatography with a chloroform/methanol/water (65:35:5, v/v/v) mobile phase. Lipids were visualized by charring with a solution containing cupric sulfate (10%, w/v) and phosphoric acid (8%, v/v) at 150 °C [36]. In all cases, a single spot was observed, confirming purity of the lipid stocks. Phospholipid aliquots were subjected to total digestion by perchloric acid, followed by a colorimetric phosphate assay for the purpose of concentration estimation [37]. DMPC, used as an internal standard,



provided an estimate of the extent of lipid digestion. All other chemicals used were of the highest purity available. Water purified through a Millipore (Bedford, MA) Milli-Q system and spectroscopy grade solvents were used throughout.

Sample Preparation

Small unilamellar vesicles (SUVs) of POPC containing 2% (mol/mol) WALP23 were used for all experiments. For this purpose, 640 nmol of POPC and 12.8 nmol of WALP23 in methanol, along with a few drops of chloroform, were mixed well by vortexing. The resultant solution was dried, while being warmed gently (~35 °C), under a stream of nitrogen. This was followed by further drying under a high vacuum for at least 3 h. Subsequently, 1.5 ml of 10 mM sodium phosphate, 150 mM sodium chloride, pH 7.2 buffer was added to the dried lipid mixture to induce swelling of the lipid film. Each hydrated lipid sample, vortexed intermittently for 3 min to ensure uniform lipid dispersion, led to the formation of homogeneous multilamellar vesicles (MLVs). These MLVs were sonicated to clarity (~60 min in short bursts) using a Sonics Vibra-Cell VCX 500 sonifier (Sonics & Materials Inc., Newtown, CT) fitted with a microtip. The lipid suspensions were purged with argon prior to sonication and cooled in an ice/water mixture during each sonication step to ensure negligible lipid damage. Titanium particles shed from the microtip during sonication were removed by centrifuging the sonicated samples in a Heraeus Biofuge centrifuge (DJB Labcare, Buckinghamshire, UK) for 15 min at 15,000 rpm. Prior to data acquisition, SUVs prepared this way were incubated for a period of 12 h in dark at room temperature (~23 °C) to ensure equilibration. A similar method was used to prepare background samples, in which the peptide was omitted. All experiments were carried out with three sets of samples at room temperature (~23 °C).

Circular Dichroism (CD) Measurements

CD measurements were carried out with a Chirascan Plus spectropolarimeter (Applied Photophysics, Surrey, UK) calibrated with (+)-10-camphorsulfonic acid [38]. Samples were scanned from 200 to 260 nm for monitoring peptide secondary structure in a quartz optical cell with a 0.1 cm path length. Spectra were recorded in wavelength increments of 0.2 nm, with a band width of 1 nm and a response time of 1 s, with a full scale sensitivity of 100 mdeg. A scan rate of 50 nm/min was used and each spectrum was the average of 10 continuous scans. Background correction of the spectra were carried out with blanks without peptide. Data are represented as mean residue ellipticities:

$$[\theta] = \theta_{\text{obs}} / (10\text{C1}) \tag{1}$$

where θ_{obs} is the observed ellipticity in mdeg, C is the concentration of peptide bonds in mol/l, and l is the path length in cm. The CD spectrum was smoothened to a moderate extent for the purpose of representation. This was done using the adjacent averaging algorithm in Microcal Origin (v8.0, OriginLab, Northampton, MA), while ensuring there is negligible change in the overall spectral shape.

Steady State Fluorescence Measurements

Steady state fluorescence data were acquired in a Fluorolog-3 Model FL3–22 spectrofluorometer (Horiba Jobin Yvon, Edison, NJ) using semi-micro quartz cuvettes, as described previously [39, 40]. Slit widths of 2.5 and 3 nm were used for excitation and emission. Spectra were recorded in the corrected spectrum mode. Data shown represent three independent measurements and in each case, the reported emission maxima were identical (or ± 1 nm of the values reported). Fluorescence anisotropy measurements were performed using Glen-Thompson polarization accessory in the same instrument and values were calculated as described previously [40]. Excitation and emission slits with slit widths of 3 nm each were used for all anisotropy measurements. Data shown are means \pm SE of three independent measurements.

Time-Resolved Fluorescence Measurements

Fluorescence lifetimes were calculated from time-resolved fluorescence intensity decays using an IBH 5000F NanoLED equipment (Horiba Jobin Yvon, Edison, NJ) with DataStation software v6.2 in the time-correlated single photon counting (TCSPC) mode, as described previously, with some modifications [40]. The excitation source was a pulsed light-emitting diode (NanoLED-295). This LED, run at a repetition rate of 1 MHz, generates optical pulses at 295 nm with pulse duration of <1.0 ns. Data were acquired using emission band pass of 6 nm or less. Intensity-averaged mean fluorescence lifetimes (<\tau>) were calculated from the extracted decay times and pre-exponential factors [41]:

$$\langle \tau \rangle = \frac{\alpha_1 \tau_1^2 + \alpha_2 \tau_2^2 + \alpha_3 \tau_3^2}{\alpha_1 \tau_1 + \alpha_2 \tau_2 + \alpha_3 \tau_3} \tag{2}$$

where α is the pre-exponential factor representing the fractional contribution to the time-resolved decay of the given component with a lifetime of τ .

Data Analysis and Plotting

Data analysis and plotting were carried out with Microcal Origin v8.0 (OriginLab, Northampton, MA).



Results and Discussion

In this work, we have monitored the organization and dynamics of the interfacial tryptophan residues of WALP23 in POPC membranes using wavelength-selective fluorescence approaches, along with CD spectroscopy. The choice of POPC bilayers was due to the fact that the hydrophobic length of POPC membranes in the fluid phase [42], matches approximately the hydrophobic length of the WALP23 transmembrane helix (see Fig. 1). Figure 2a shows a representative fluorescence emission spectrum of WALP23 in POPC membranes. The wavelength of emission maximum is 333 nm, consistent with the location of the tryptophan residues in a solvent inaccessible membrane environment. Figure 2b shows a representative far-UV CD spectrum of WALP23 in POPC membranes which corresponds to a predominantly α -helical conformation, in agreement with previous reports [43].

Wavelength-selective fluorescence (including REES) is a phenomenon observed with polar fluorophores in an environment characterized by motional restriction, for example, in membranes or proteins [31–34]. A crucial prerequisite for the observation of

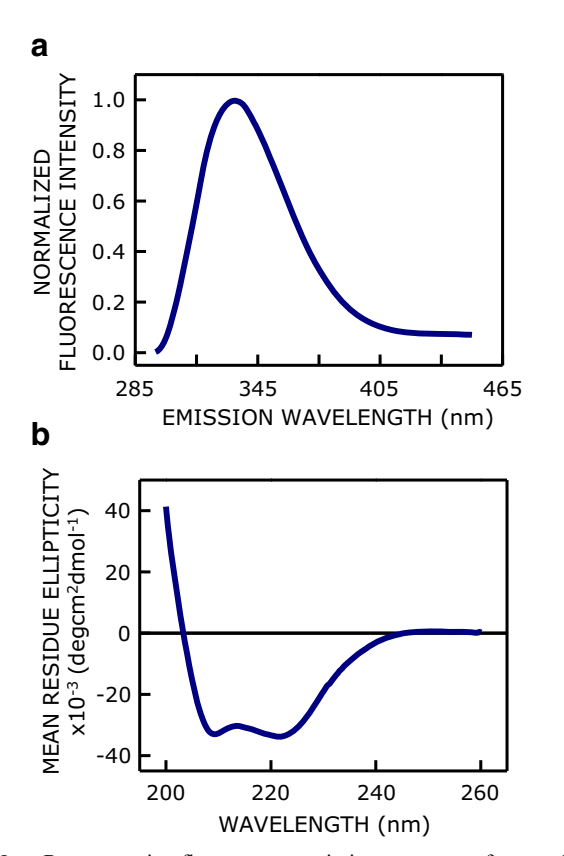


Fig. 2 a Representative fluorescence emission spectrum of tryptophan residues in WALP23 in POPC vesicles. The fluorescence spectrum, acquired at an excitation wavelength of 280 nm, was intensity-normalized at the emission maximum (333 nm). b Representative far-UV CD spectrum of WALP23 in POPC vesicles. The concentration of WALP23 was 8.5 μM and the peptide to lipid ratio was 1:50 (mol/mol) in both cases. See Experimental for more details

REES is that the time scale associated with solvent relaxation in the fluorophore microenvironment should be slower than or comparable to the fluorescence lifetime (usually ns). This results in the coupling of solvation dynamics to the local dynamics of the fluorophore in the excited state. The coupling allows REES to explore the organization and dynamics of fluorophores in restricted environments such as the membrane interface. REES is operationally defined as the shift in the emission maximum of a fluorophore toward longer wavelengths, due to a concomitant shift in the excitation wavelength toward the red edge of the absorption spectrum. The change in the wavelength of maximum fluorescence emission of the tryptophan residues (residues 2, 3, 21, 22; see Fig. 1) in WALP23 in POPC membranes with increase in the excitation wavelength is shown in Fig. 3a. The figure shows that the emission maximum shifts from 333 to

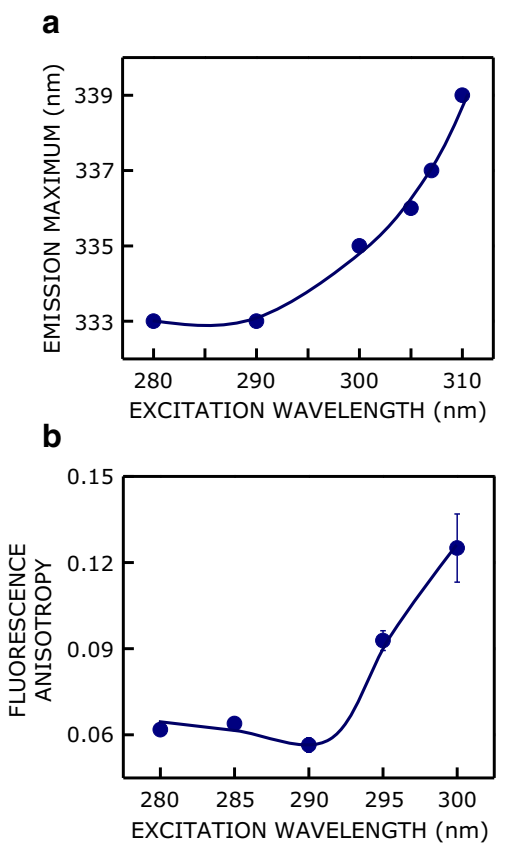


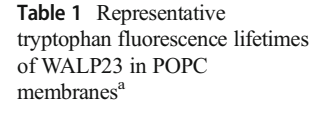
Fig. 3 Wavelength-selective fluorescence of WALP23 in POPC membranes. a Red shift in the wavelength of maximum emission of WALP23 in POPC membranes, upon increasing the excitation wavelength. The magnitude of REES, operationally defined as the total shift in fluorescence emission maximum upon changing the excitation wavelength from 280 to 310 nm, was 6 nm. Data shown represents three independent measurements and the observed emission maxima were identical or within ± 1 nm of the values reported. b Change in fluorescence anisotropy of WALP23 with increasing excitation wavelength. The emission wavelength was 333 nm. Data represent means \pm SE of three independent measurements. The line joining the data points is provided as a viewing guide. The concentration of WALP23 was 8.5 μ M and the peptide to lipid ratio was 1:50 (mol/mol) in both cases. See Experimental for more details



339 nm, in response to increase in excitation wavelength from 280 to 310 nm. The shift amounts to REES of 6 nm and indicates that the interfacial tryptophan residues of WALP23, on the average, experience a motionally restricted microenvironment.

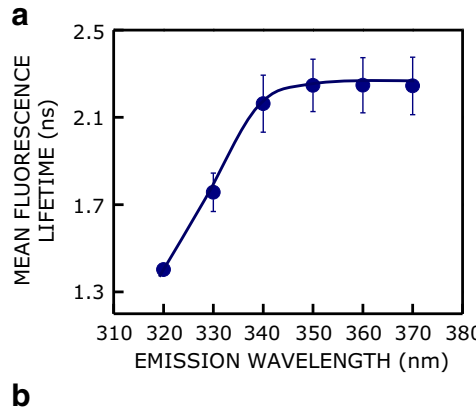
Another manifestation of motionally restricted environment is the wavelength-dependence of fluorescence anisotropy [31]. Figure 3b shows the increase in fluorescence anisotropy with excitation wavelength of WALP23 in POPC membranes. The figure shows that the fluorescence anisotropy displays a substantial increase (~102%) with increase in the excitation wavelength from 280 to 300 nm, with a pronounced enhancement beyond 290 nm. We found it difficult to acquire data beyond 300 nm due to scattering artifacts and poor signal-to-noise ratio. This excitation wavelength dependent shift in fluorescence anisotropy is characteristic for tryptophans in restricted environments such as the membrane interface [44]. The increased fluorescence anisotropy at the red edge originates from solvent-relaxed fluorophores (the subpopulation photoselected on red edge excitation) in which rotational dynamics of the fluorophore is restricted by the surrounding solvent molecules via strong dipolar interactions [31]. The slight dip in anisotropy at 290 nm deserves comment. This dip is typical of tryptophans localized at the membrane interface [44] and has its genesis in the complex photophysics of the overlapping, mutually orthogonal So-SI electronic transitions (¹L_a and ¹L_b) of tryptophan [31, 34, 44].

As mentioned above, the photophysical principle underlying REES is the photoselection of a fluorophore subpopulation in the excited state on red edge excitation, which gives rise to varying extents of solvent relaxation at each excitation wavelength. Since fluorescence lifetime is sensitive to the fluorophore microenvironment [45], varying extents of solvent relaxation around a fluorophore results in changes in lifetime. Figure 4a shows the emission wavelength dependence of the mean fluorescence lifetime of WALP23 tryptophans in POPC membranes. The mean fluorescence lifetimes at different emission wavelengths are shown in Table 1. Intensity-averaged mean fluorescence lifetime is the



Emission wavelength (nm)	α_1	τ_1 (ns)	α_2	τ_2 (ns)	α_3	τ_3 (ns)	$<\tau>$ b (ns)	χ^2
320	0.03	1.38	0.96	0.07	0.01	3.75	1.39	1.2
330	0.05	1.53	0.94	0.06	0.01	4.25	1.72	1.4
340	0.50	1.61	0.44	0.29	0.06	4.44	2.10	1.4
350	0.53	1.84	0.42	0.60	0.05	5.06	2.18	1.4
360	0.57	1.79	0.37	0.69	0.06	4.80	2.16	1.3
370	0.60	1.73	0.33	0.62	0.07	4.70	2.21	1.3

 $[^]a$ The excitation wavelength was 295 nm. A total of 10,000 photons were collected at the peak channel for robust data acquisition. The concentration of WALP23 was 8.5 μM and the peptide to lipid ratio was 1:50 (mol/mol). See Experimental for more details



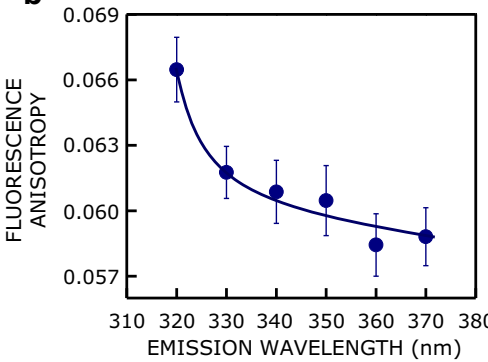


Fig. 4 Emission wavelength dependent fluorescence properties of WALP23 in POPC vesicles. **a** Effect of increasing emission wavelength on the mean intensity-averaged fluorescence lifetime of WALP23 in POPC membranes. The excitation wavelength was 295 nm. Mean fluorescence lifetimes were calculated using Eq. (2). **b** Reduction in fluorescence anisotropy with increasing emission wavelength. Excitation wavelength was kept constant at 280 nm. The line joining the data points is provided as a viewing guide. Data represent means \pm SE of three independent measurements. The concentration of WALP23 was 8.5 μM and the peptide to lipid ratio was 1:50 (mol/mol) in both cases. See Experimental for more details

parameter of choice due to the fact that it does not depend on the type of analysis employed or the number of exponential terms used to deconvolute the time-resolved fluorescence decay. A representative decay profile of WALP23 tryptophans in POPC membranes is shown in Fig. S1. Figure 4a shows that

^b Calculated using Eq. (2)

the mean fluorescence lifetime displays a substantial increase (~60%) with increasing emission wavelength in the range of 320 to 370 nm. Emission at shorter wavelengths photoselects unrelaxed fluorophores. The unrelaxed subpopulation of fluorophores undergoes relaxation in two different ways, by fluorescence emission at the given excitation wavelength and by decay to longer wavelengths (that remain unobserved). This dual mode of relaxation leads to shorter lifetimes in the excited state. On the other hand, fluorophore populations emitting at the longer wavelengths are more relaxed due to a longer time spent in the excited state, corresponding to longer fluorescence lifetimes, thereby allowing greater extents of solvent relaxation. Figure 4b shows the decrease in fluorescence anisotropy (~12%) with increasing emission wavelength. Longer-lived fluorophores, photoselected at longer emission wavelengths, are associated with greater extents of rotation in the excited state. This leads to lower values of fluorescence anisotropy at the red edge due to greater depolarization.

Taken together, our results show that the tryptophan residues in the α -helical WALP23 peptide in POPC membranes experience constrained rotational dynamics. Since WALP23 has four tryptophans, these results correspond to the average environment experienced by the tryptophans. These observations assume relevance in light of existing literature on the strong correlation of tryptophan solvation dynamics to the presence of functionally active conformations in membrane proteins and peptides [13, 14, 27–30, 46]. We envision these results could be useful in future studies employing fluorescence spectroscopy on the crucial role of tryptophan localization and dynamics in the membrane conformation and orientation of WALP analogs, and their subsequent response to mismatch conditions in a membrane milieu.

Acknowledgments This work was supported by intramural research grants from the Council of Scientific and Industrial Research, Govt. of India. A.C. gratefully acknowledges support from SERB Distinguished Fellowship (Department of Science and Technology, Govt. of India). R.E.K. acknowledges support from MCB grant 1713242 from the United States National Science Foundation. S.P. thanks the University Grants Commission for the award of a Senior Research Fellowship. We thank members of the Chattopadhyay laboratory for their comments and discussions.

Compliance with Ethical Standards

Conflict of Interest The authors declare that they have no conflict of interest.

References

- Killian JA (2003) Synthetic peptides as models for intrinsic membrane proteins. FEBS Lett 555:134–138
- Killian JA, Salemink I, de Planque MRR, Lindblom G, Koeppe II RE, Greathouse DV (1996) Induction of nonbilayer structures in diacylphosphatidylcholine model membranes by transmembrane

- α -helical peptides: importance of hydrophobic mismatch and proposed role of tryptophans. Biochemistry 35:1037–1045
- Vostrikov VV, Koeppe II RE (2011) Response of GWALP transmembrane peptides to changes in the tryptophan anchor positions. Biochemistry 50:7522–7535
- Vostrikov VV, Daily AE, Greathouse DV, Koeppe II RE (2010) Charged or aromatic anchor residue dependence of transmembrane peptide tilt. J Biol Chem 285:31723–31730
- van't Hag L, Li X, Meikle TG, Hoffmann SV, Jones NC, Pedersen JS, Hawley AM, Gras SL, Conn CE, Drummond CJ (2016) How peptide molecular structure and charge influence the nanostructure of lipid bicontinuous cubic mesophases: model synthetic WALP peptides provide insights. Langmuir 32:6882–6894
- Killian JA (1992) Gramicidin and gramicidin-lipid interactions. Biochim Biophys Acta 1113:391

 –425
- Koeppe II RE, Andersen OS (1996) Engineering the gramicidin channel. Annu Rev Biophys Biomol Struct 25:231–258
- Kelkar DA, Chattopadhyay A (2007) The gramicidin ion channel: a model membrane protein. Biochim Biophys Acta 1768:2011–2025
- Arkin IT, Brunger AT (1998) Statistical analysis of predicted transmembrane α-helices. Biochim Biophys Acta 1429:113–128
- Adamian L, Nanda V, DeGrado WF, Liang J (2005) Empirical lipid propensities of amino acid residues in multispan alpha helical membrane proteins. Proteins 59:496–509
- Strandberg E, Özdirekcan S, Rijkers DTS, van der Wel PCA, Koeppe II RE, Liskamp RMJ, Killian JA (2004) Tilt angles of transmembrane model peptides in oriented and non-oriented lipid bilayers as determined by ²H solid-state NMR. Biophys J 86:3709– 3721
- van der Wel PCA, Strandberg E, Killian JA, Koeppe II RE (2002) Geometry and intrinsic tilt of a tryptophan-anchored transmembrane alpha-helix determined by ²H NMR. Biophys J 83:1479– 1488
- Schiffer M, Chang C-H, Stevens FJ (1992) The functions of tryptophan residues in membrane proteins. Protein Eng 5:213–214
- Kelkar DA, Chattopadhyay A (2006) Membrane interfacial localization of aromatic amino acids and membrane protein function. J Biosci 31:297–302
- Mouritsen OG, Bloom M (1984) Mattress model of lipid-protein interactions in membranes. Biophys J 46:141–153
- Killian JA (1998) Hydrophobic mismatch between proteins and lipids in membranes. Biochim Biophys Acta 1376:401–416
- Dumas F, Lebrun MC, Tocanne J-F (1999) Is the protein/lipid hydrophobic matching principle relevant to membrane organization and functions? FEBS Lett 458:271–277
- Andersen OS, Koeppe II RE (2007) Bilayer thickness and membrane protein function: an energetic perspective. Annu Rev Biophys Biomol Struct 36:107–130
- Rao BD, Shrivastava S, Chattopadhyay A (2017) Hydrophobic mismatch in membranes: when the tail matters. In: Chattopadhyay A (ed) Membrane organization and dynamics. Springer, Heidelberg, pp 375–387
- van der Wel PCA, Pott T, Morein S, Greathouse DV, Koeppe II RE, Killian JA (2000) Tryptophan-anchored transmembrane peptides promote formation of nonlamellar phases in phosphatidylethanolamine model membranes in a mismatch-dependent manner. Biochemistry 39:3124–3133
- Morein S, Koeppe II RE, Lindblom G, de Kruijff B, Killian JA (2000) The effect of peptide/lipid hydrophobic mismatch on the phase behavior of model membranes mimicking the lipid composition in *Escherichia coli* membranes. Biophys J 78:2475–2485
- de Planque MRR, Bonev BB, Demmers JAA, Greathouse DV, Koeppe II RE, Separovic F, Watts A, Killian JA (2003) Interfacial anchor properties of tryptophan residues in transmembrane peptides can dominate over hydrophobic matching effects in peptide-lipid interactions. Biochemistry 42:5341–5348



- de Planque MRR, Kruijtzer JAW, Liskamp RMJ, Marsh D, Greathouse DV, Koeppe II RE, de Kruijff B, Killian JA (1999) Different membrane anchoring positions of tryptophan and lysine in synthetic transmembrane α-helical peptides. J Biol Chem 274: 20839–20846
- 24. de Planque MRR, Boots J-WP, Rijkers DTS, Liskamp RMJ, Greathouse DV, Killian JA (2002) The effects of hydrophobic mismatch between phosphatidylcholine bilayers and transmembrane α-helical peptides depend on the nature of interfacially exposed aromatic and charged residues. Biochemistry 41:8396–8404
- Özdirekcan S, Rijkers DTS, Liskamp RMJ, Killian JA (2005) Influence of flanking residues on tilt and rotation angles of transmembrane peptides in lipid bilayers. A solid-state ²H NMR study. Biochemistry 44:1004–1012
- Mortazavi A, Rajagopalan V, Sparks KA, Greathouse DV, Koeppe II RE (2016) Juxta-terminal helix unwinding as a stabilizing factor to modulate the dynamics of transmembrane helices. ChemBioChem 17:462–465
- Ghosh AK, Rukmini R, Chattopadhyay A (1997) Modulation of tryptophan environment in membrane-bound melittin by negatively charged phospholipids: implications in membrane organization and function. Biochemistry 36:14291–14305
- Rawat SS, Kelkar DA, Chattopadhyay A (2004) Monitoring gramicidin conformations in membranes: a fluorescence approach. Biophys J 87:831–843
- Chattopadhyay A, Rawat SS, Greathouse DV, Kelkar DA, Koeppe II RE (2008) Role of tryptophan residues in gramicidin channel organization and function. Biophys J 95:166–175
- Chaudhuri A, Haldar S, Sun H, Koeppe RE II, Chattopadhyay A (2014) Importance of indole N-H hydrogen bonding in the organization and dynamics of gramicidin channels. Biochim Biophys Acta 1838:419–428
- Mukherjee S, Chattopadhyay A (1995) Wavelength-selective fluorescence as a novel tool to study organization and dynamics in complex biological systems. J Fluoresc 5:237–246
- Demchenko AP (2008) Site-selective red-edge effects. Methods Enzymol 450:59–78
- Haldar S, Chaudhuri A, Chattopadhyay A (2011) Organization and dynamics of membrane probes and proteins utilizing the red edge excitation shift. J Phys Chem B 115:5693–5706

- Chattopadhyay A, Haldar S (2014) Dynamic insight into protein structure utilizing red edge excitation shift. Acc Chem Res 47:12–19
- Gleason NJ, Vostrikov VV, Greathouse DV, Grant CV, Opella SJ, Koeppe II RE (2012) Tyrosine replacing tryptophan as an anchor in GWALP peptides. Biochemistry 51:2044–2053
- Baron CB, Coburn RF (1984) Comparison of two copper reagents for detection of saturated and unsaturated neutral lipids by charring densitometry. J Liq Chromatogr 7:2793–2801
- McClare CWF (1971) An accurate and convenient organic phosphorus assay. Anal Biochem 39:527–530
- Chen GC, Yang JT (1977) Two-point calibration of circular dichrometer with d-10-camphorsulfonic acid. Anal Lett 10:1195– 1207
- Chakraborty H, Chattopadhyay A (2017) Sensing tryptophan microenvironment of amyloid protein utilizing walvelength-selective fluorescence approach. J Fluoresc 27:1995–2000
- Rao BD, Chakraborty H, Keller S, Chattopadhyay A (2018) Aggregation behavior of pHLIP in aqueous solution at low concentrations: a fluorescence study. J Fluoresc 28:967–973
- Lakowicz JR (2006) Principles of fluorescence spectroscopy. 3rd edn. Springer, New York
- Kučerka N, Nieh M-P, Katsaras J (2011) Fluid phase lipid areas and bilayer thicknesses of commonly used phosphatidylcholines as a function of temperature. Biochim Biophys Acta 1808:2761–2771
- de Planque MRR, Goormaghtigh E, Greathouse DV, Koeppe II RE, Kruijtzer JAW, Liskamp RMJ, de Kruijff B, Killian JA (2001) Sensitivity of single membrane-spanning α-helical peptides to hydrophobic mismatch with a lipid bilayer: effects on backbone structure, orientation, and extent of membrane incorporation. Biochemistry 40:5000–5010
- Mukherjee S, Chattopadhyay A (1994) Motionally restricted tryptophan environments at the peptide-lipid interface of gramicidin channels. Biochemistry 33:5089–5097
- 45. Prendergast FG (1991) Time-resolved fluorescence techniques: methods and applications in biology. Curr Opin Struct Biol 1: 1054-1059
- Pal S, Aute R, Sarkar P, Bose S, Deshmukh MV, Chattopadhyay A (2018) Constrained dynamics of the sole tryptophan in the third intracellular loop of the serotonin_{1A} receptor. Biophys Chem 240: 34–41

